

Axon tracts guide zebrafish facial branchiomotor neuron migration through the hindbrain

Sarah J. Wanner and Victoria E. Prince*

SUMMARY

Appropriate localization of neurons within the brain is a crucial component of the establishment of neural circuitry. In the zebrafish hindbrain, the facial branchiomotor neurons (FBMNs) undergo a chain-like tangential migration from their birthplace in rhombomere (r) 4 to their final destination in r6/r7. Here, we report that ablation of either the cell body or the trailing axon of the leading FBMN, or 'pioneer' neuron, blocks the migration of follower FBMNs into r5. This demonstrates that the pioneer neuron and its axon are crucial to the early migration of FBMNs. Later migration from r5 to r6 is not dependent on pioneer neurons but on the medial longitudinal fasciculus (MLF), a bundle of axons lying ventral to the FBMNs. We find that MLF axons enter r5 only after the pioneer neuron has led several followers into this region; the MLF is then contacted by projections from the FBMNs. The interactions between FBMNs and the MLF are important for migration from r5 to r6, as blocking MLF axons from entering the hindbrain can stall FBMN migration in r5. Finally, we have found that the adhesion molecule Cdh2 (N-cadherin) is important for interactions between the MLF and FBMNs, as well as for interactions between the trailing axon of the pioneer neuron and follower FBMNs. Interestingly, migration of pioneer neurons is independent of both the MLF and Cdh2, suggesting pioneer migration relies on independent cues.

KEY WORDS: Facial branchiomotor neurons, Neuron migration, Cdh2, Zebrafish

INTRODUCTION

Migration of neurons from their birthplace to their final destination is central to the formation and proper wiring of nervous system circuitry. Understanding how neurons successfully navigate to their proper targets is important because defects in neuronal migration can result in human neurological diseases (Ross and Walsh, 2001; Valiente and Marín, 2010). Many neurons undergo radial migration outwards from their birthplace in the ventricular zone, with the migrations that establish the complex layered structure of the cortex providing a familiar example (Hatten, 1999; Nadarajah and Parnavelas, 2002). A subset of neurons also undergoes tangential migrations perpendicular to the plane of the neuroepithelium; examples include the rostral migratory neurons of the olfactory bulb, the granule neurons of the cerebellum and the facial branchiomotor neurons of the hindbrain (Hatten, 1999; Chandrasekhar, 2004).

The facial branchiomotor neurons (FBMNs) of the VIIth nerve reside within the hindbrain and control the muscles of facial expression and other pharyngeal arch II-derived structures. These neurons undergo a simple, stereotypical posterior tangential migration that is conserved in humans, mice and zebrafish (Chandrasekhar, 2004). In zebrafish, the first FBMNs are born at 16 hours post fertilization (hpf) in the ventral aspect of hindbrain rhombomere (r) 4. The cell bodies then migrate tangentially, moving posteriorly in a chain-like manner to their destinations in r6 and r7 (Chandrasekhar, 2004; Song, 2007). The first FBMN to migrate reaches r6 around 20 hpf and migration of all FBMNs is complete by 48 hpf. Although multiple proteins have been identified that are important for this migration, including planar cell polarity (PCP)

components (reviewed by Wada and Okamoto, 2009a; Wada and Okamoto, 2009b) and adhesion factors (Garel et al., 2000; Sittaramane et al., 2009; Grant and Moens, 2010; Stockinger et al., 2011), the possibility that FBMNs follow environmental cues such as pre-existing axon tracts though the hindbrain remains largely unexplored.

In the case of the FBMNs, there are two pre-existing axon tracts that could potentially guide their migration. First, as each FBMN migrates, it leaves behind a trailing axon, and these collectively exit the neural tube at r4 to innervate pharyngeal arch II (Chandrasekhar, 2004). The trailing axon laid down by the first FBMN to migrate could serve as a guide for subsequent FBMNs to follow. Second, FBMNs migrate in close proximity to the axons of the medial longitudinal fasciculus (MLF) and this structure could guide their migration into r6. The MLF is one of the first axon tracts to develop in zebrafish, emanating from clustered ventral cell bodies in the midbrain that make up the nucleus of the MLF (nMLF). nMLF interneurons extend long axon projections posteriorly within the ventral CNS, beginning around 16 hpf; these axons fasciculate to form the MLF (Chitnis and Kuwada, 1990; Ross et al., 1992). FBMNs appear to migrate in close proximity to this axon tract and have been shown to contact the MLF directly at 24 hpf (Wada et al., 2006), suggesting this fasciculus could function as a guide to the FBMNs.

Interactions between FBMNs and pre-existing axon tracts would depend upon cell-cell contact regulated by cell adhesion factors. Recently, the cell-adhesion molecule Cdh2 (N-cadherin) has been shown to regulate both FBMN cohesion and neuroepithelial cell cohesion, and depletion of Cdh2 dramatically disrupts FBMN migration (Stockinger et al., 2011). Cdh2 is expressed broadly throughout the vertebrate nervous system and mutant analysis indicates this molecule functions in multiple aspects of neuroepithelium and neural tube development (Hatta and Takeichi, 1986; Radice et al., 1997; Gänzler-Odenthal and Redies, 1998; Lele et al., 2002; Hong and Brewster, 2006). The importance of Cdh2 in FBMN migration suggests Cdh2 may be required for regulating

Department of Organismal Biology and Anatomy, The University of Chicago, 1027 East 57th Street, Chicago, IL 60637, USA.

*Author for correspondence (vprince@uchicago.edu)

adhesion between FBMNs and pre-existing axon tracts in the hindbrain environment, enabling FBMNs to migrate to their destination.

Here, we show that tangential FBMN migration proceeds via a two-phase process. The early phase of migration from the birthplace of the FBMNs in r4 to r5 is regulated by a 'pioneer' neuron; the first neuron to migrate on each side of the hindbrain leads follower FBMNs into r5. By contrast, the second phase of migration from r5 to r6 is dependent upon interactions with the underlying MLF axon tract. Both of these interactions involve the cell-adhesion molecule Cdh2. However, migration of pioneer neurons requires neither Cdh2 nor interactions with the MLF, suggesting that pioneer neurons migrate using a separate mechanism to all other FBMNs.

MATERIALS AND METHODS

Fish lines and husbandry

Zebrafish were maintained following standard procedures. Embryos were maintained at 28.5°C and staged as described previously (Kimmel et al., 1995). Transgenic lines were used as described: Tg(*HuC*:GFP) (Park et al., 2000), Tg(*islet1*:GFP) (Higashijima et al., 2000), Tg(pGFP5.3) (Picker et al., 2002) and Tg(*zCREST1*:membrFP) (Mapp et al., 2010).

Morpholino design and microinjection

A translation-blocking morpholino (MO; Gene Tools) was designed to target the Cdh2 5'UTR (5'-TCTGTATAAAGAAACCGATAGAGTT-3') as described by Lele et al. (Lele et al., 2002). The MO was dissolved to a stock concentration of 1 mM and injected into one- to two-cell stage embryos at a concentration of 100 µM.

Immunohistochemistry and sectioning

Embryos were fixed overnight in 4% paraformaldehyde and immunohistochemistry was performed as described previously (Prince et al., 1998) using the following primary antibodies: zn-12 (1:500; DSHB), RFP (1:500; Chemicon), GFP-Alexa488 (1:500; Molecular Probes) and HuC/D (1:500; Molecular Probes). Transverse sectioning was performed on a Vibratome Series 1000 Plus Tissue Sectioning System, producing 100–150 µm slices.

MLF surgical block

Tg(*zCREST1*:membrFP) embryos were placed into explant media (Bingham et al., 2005) containing L15 media (Gibco), 1 M glucose (Sigma) and pen/strep (Sigma) in a depression slide and oriented in 2% methylcellulose. The brain was severed at r2 using a set of Lumsden BioScissors (Oban Precision Instruments) at 14 hpf. Severed embryos were removed from the methylcellulose, placed in a Petri dish containing explant media, grown to 22 hpf at 28.5°C and fixed in 4% paraformaldehyde for immunohistochemistry and analysis.

Ablations

Embryos were anesthetized with tricaine and embedded in 0.8% agarose on a 35 mm imaging Petri dish (MatTek). The two-photon laser on a Leica SP5 Tandem Scanner Spectral 2-Photon confocal microscope was used to ablate one *islet1*:GFP-positive neuron, pGFP5.3-positive neuroepithelial cell or *zCREST1*:membrFP-positive pioneer axon on one side of the embryo. Embryos from each ablation experimental group were imaged from 19–21 hpf for time-lapse analysis. After time-lapse imaging, embryos were removed from the agarose, grown to 24 hpf at 28.5°C and fixed with 4% paraformaldehyde for immunohistochemistry and analysis.

Microscopy and data analysis

Fixed embryos were imaged on Zeiss LSM 510 and LSM 710 laser scanning confocal microscopes. Time-lapse imaging of living embryos was performed on a Zeiss LSM 510 confocal microscope; time-lapse imaging of ablation experiments was performed on a Leica SP5 Tandem Scanner Spectral 2-Photon confocal microscope. For all time-lapse movies, each time point represents a *z*-stack projection taken at 5-minute intervals. Movies were recorded for 2 hours to ensure that immersion objective water did not evaporate. Data were analyzed using ImageJ (NIH). Unpaired two-

tailed *t*-test statistical analysis was performed using Prism (GraphPad). Average speed was measured by marking the position of each FBMN at each 5-minute time-lapse time point. Average posterior velocity was measured by marking the position of each FBMN at the start of the time-lapse and again either when the MLF had caught up with the neuron or at the end of the time-lapse. The average number of protrusions was measured by counting the number of protrusions present on each neuron at each 5-minute time point. The average length of protrusions was obtained by measuring the length of each protrusion during each 5-minute time point. The average angle of protrusion was obtained by measuring the angle of each protrusion per 5-minute time point, where 0° is in the direction of posterior movement and 90° is towards the midline.

RESULTS

The MLF is not required for early migration of FBMNs from r4 to r5

The medial longitudinal fasciculus (MLF) has previously been hypothesized to function as a guide to FBMNs migrating tangentially through the hindbrain. Wada and colleagues (Wada et al., 2006) showed that FBMNs interact directly with the MLF at 24 hpf. We confirmed and extended this observation using Tg(*zCREST1*:membrFP) zebrafish embryos immunolabeled with zn-12 antibody to visualize the FBMNs (red; Mapp et al., 2010) and the MLF (Fig. 1, green, white arrowheads); the zn-12 antibody labels a subset of early axon pathways, including both the MLF and lateral longitudinal fasciculus (LLF, yellow arrowheads) (Metcalf et al., 1990), which lies lateral to the MLF. Tg(*zCREST1*:membrFP) also labels a few cells of the otic vesicle (Fig. 1A, asterisks) (Mapp et al., 2010); however, this did not detract from our ability to image FBMNs. We found that during early (20 hpf) and later (22 and 24 hpf) stages of FBMN migration, FBMNs migrate in close apposition to the MLF (Fig. 1A–C). Transverse sections at r5 revealed direct interaction between FBMNs and the MLF at each stage (Fig. 1D–F). Our findings are consistent with previous reports and additionally establish that FBMNs contact the MLF at minimum between the stages of 20 and 28 hpf (Fig. 1 and data not shown).

To examine the interaction between the MLF and FBMNs in greater detail, we performed *in vivo* time-lapse confocal microscopy on double transgenic embryos (Fig. 2; supplementary material Movie S1). Tg(*zCREST1*:membrFP) labels FBMNs (red), whereas Tg(*HuC*:GFP) labels all differentiated neurons, including the MLF and its axons (green; Park et al., 2000). Our time-lapse analysis demonstrated that the first MLF axon (arrowhead) did not enter r4 until 18–18.5 hpf, by which time several FBMNs had already migrated into r5 (Fig. 2A). The first MLF axon did not reach r6 until around 19.5–20 hpf, by which stage the first FBMN to migrate (arrow) had already reached r6 and several FBMNs had migrated into r5 (Fig. 2C). Axons of the Mauthner and other reticulospinal (RS) neurons also contribute to the MLF, and could potentially play a role in guiding FBMN migration. Although the r4-localized Mauthner neuron initiates axon outgrowth at 17.5 hpf, its axon does not cross the midline until 18–19 hpf, before turning posteriorly to contribute to the MLF at 21–22 hpf (Kimmel et al., 1990; Mendelson, 1986) (supplementary material Fig. S1). Other RS neuron axons similarly contribute to the MLF around 21–22 hpf (Mendelson, 1986) (supplementary material Fig. S1). Thus, these RS axons do not contribute to the relevant r4–r6 region of the MLF until after the first FBMNs have already reached r6. Together, these results indicate that early phase migration of FBMNs (from 18–20 hpf) cannot require the MLF or RS axons, as these structures are not physically present in the relevant location during these stages.

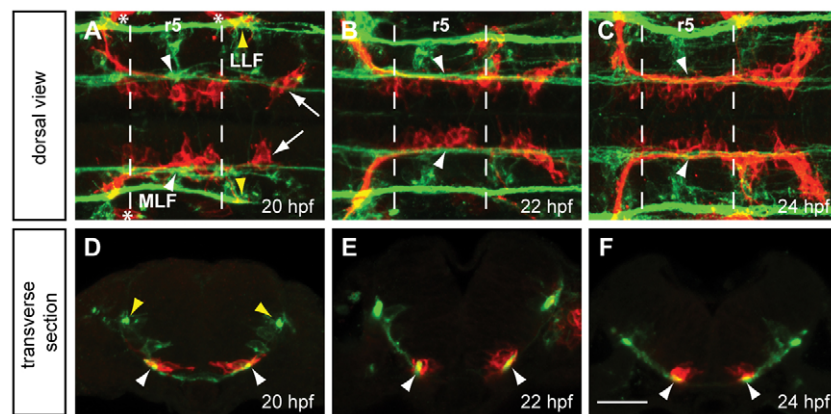


Fig. 1. FBMNs migrate in close apposition to the MLF. (A–C) Maximum projection dorsal views of *Tg(zCREST1:membRFP)* embryos immunostained using zn-12 antibody show that FBMNs lie in close proximity to the MLF throughout their migration. zn-12 (green) labels the MLF (white arrowheads) and lateral longitudinal fasciculus (LLF, yellow arrowheads). (A) At 20 hpf, FBMNs (red) have migrated into r5 and the first FBMNs to migrate have reached r6 (arrows). (B) By 22 hpf, migration has continued with more FBMNs reaching r6. (C) At 24 hpf, FBMN migration into r6 continues. (D–F) Transverse sections of *zCREST1:membRFP* embryos at r5 stained using zn-12 show direct interaction between the MLF and FBMNs (white arrowheads) throughout FBMN migration at (D) 20 hpf, (E) 22 hpf and (F) 24 hpf. Asterisks highlight the otic vesicle. Broken lines indicate r5 boundaries for all figures. Scale bar: 20 μ m.

The MLF is required for FBMN migration from r5 to r6

To examine a potential role for the MLF during the later stage of FBMN migration, as neurons proceed from r5 into r6 at ~20–22 hpf, we surgically blocked MLF axons from entering the hindbrain. Our approach was similar to methodology previously developed in chick embryos (Hernández-Montiel et al., 2003). We transected the hindbrain of *Tg(zCREST1:membRFP)* embryos at the r2 level at 14 hpf, a stage that precedes extension of MLF axons into the hindbrain. Using this approach, MLF axons were physically blocked from extending into r4 and more posterior regions of the hindbrain. The manipulated *Tg(zCREST1:membRFP)* embryos were fixed at 22 hpf and labeled with zn-12 antibody to assay FBMN migration (red) in the absence of the MLF (Fig. 3, green). Although the manipulation could effectively block MLF axons from entering the hindbrain (Fig. 3E), the region remained intact and anterior-posterior patterning was not disrupted. The r4 marker *hoxb1a*, and the r3/5 marker *krox20*, showed normal expression, indicating that anterior-posterior patterning of the r4–r6 hindbrain region was not affected by the manipulation (supplementary material Fig. S2A–D). Furthermore, the number and organization of neurons within the hindbrain showed only minor alterations after transection of the anterior hindbrain (supplementary material Fig. S2E,F).

In unmanipulated control embryos, analysis at 22 hpf showed that FBMNs migrated in close proximity to the MLF and several FBMNs had already migrated into r6 at this stage (Fig. 3A,F). When the MLF was successfully blocked from entering the hindbrain, FBMNs were unable to migrate out of r5 in 33% of embryos (Fig. 3E,F). In the remaining 67% of MLF-deficient embryos, FBMNs migrated into r6 and appeared to do so by coming into close contact with other axon tracts in the hindbrain (Fig. 3D,F). These included the LLF (white arrowheads), which remained intact in a subset of our manipulated specimens, and the projections of the RS neurons (Fig. 3D', yellow arrowheads). This intriguing result implies that the MLF is important for migration from r5 to r6, but in the absence of this axon tract the FBMNs use other local tracts to

migrate through the hindbrain. When manipulated embryos were examined later at 30 hpf, most embryos exhibited migration of FBMNs along RS neuron projections (data not shown). As noted above, these RS neuron projections normally contribute to the MLF (Fig. 3D', arrow) (Kimmel et al., 1982). To control for the possibility that simply severing the neural tube disrupted FBMN migration, embryos were transected posterior to the hindbrain at the level of somite one. The FBMNs of posteriorly transected embryos migrated normally (Fig. 3B,F). Additionally, incomplete transections at the level of r2, which left the MLF intact yet severed a very significant part of the neural tube, also resulted in normal FBMN migration (Fig. 3C,F). Together, these results establish that an intact MLF plays an important role in facilitating FBMN migration from r5 into r6; however, in the absence of the MLF, FBMNs are frequently able to migrate on other nearby axon tracts within the hindbrain.

The first FBMN to migrate acts as a pioneer neuron

The first FBMN to migrate on each side of the hindbrain often migrates far ahead of the following FBMNs and appears to send out more and longer projections into the neuroepithelial environment (Fig. 4; supplementary material Movie S2). This cellular behavior led us to hypothesize that the first FBMN to migrate may act as a 'pioneer' neuron to lead follower neurons through the hindbrain, a model previously suggested by our group and others (Rohrschneider et al., 2007; Sittaramane et al., 2009). To test this idea, we analyzed time-lapse confocal movies of FBMN migration in *Tg(zCREST1:membRFP)* embryos and found significant differences in the properties of the first FBMN to migrate (the pioneer neuron) versus follower FBMNs. We examined both early stages of FBMN migration, before the MLF catches up with the FBMNs (18–20 hpf; Fig. 4A–E), and later stages of migration, after the MLF has overtaken the FBMNs (20–22 hpf). We found that the average posteriorwards velocity, measured as the net posterior distance traveled, of pioneer neurons was lower than that of follower neurons at either stage (Fig. 4G). Average speed, measured as the total distance traveled in any direction, showed a similar trend, although

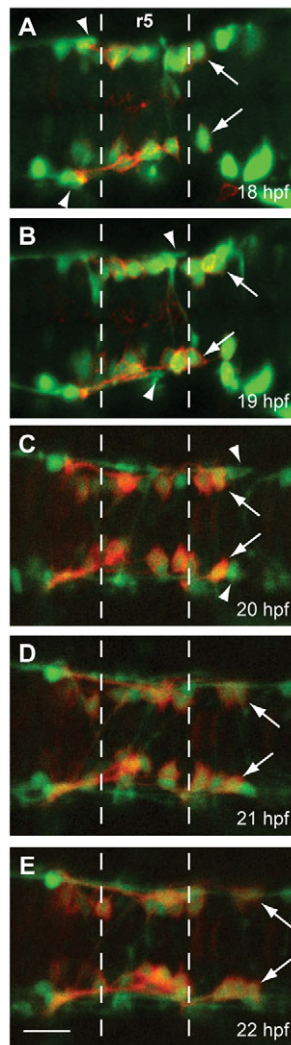


Fig. 2. FBMN migration into r5 and r6 precedes the MLF entering the r4-r6 hindbrain region. Time-lapse imaging of *Tg(zCREST1:membRFP/HuC-GFP)* embryos from 18–22 hpf. (A–E) Still images taken at 1-hour intervals from two representative time-lapse movies: (A,B) a 18–20 hpf movie; (C–E) a 20–22 hpf movie. Arrows indicate the first FBMN to migrate. Arrowheads indicate the growth cone of the first MLF axon to enter the hindbrain. Scale bar: 20 μ m.

this result was not significant (Fig. 4F). Notably, at the stage when the MLF overtakes the pioneer neurons, pioneer speed and velocity were further reduced; this is similar to the affect of the MLF on follower FBMNs (Fig. 4F,G). Pioneer neuron protrusion dynamics also showed significant differences when compared with follower neurons. Pioneer neurons had an increased average number of protrusions (Fig. 4H) and length of protrusions (Fig. 4I), suggesting that these neurons are actively exploring the environment. Once the MLF had overtaken the pioneers, protrusion number and length values decreased, hinting that there is no longer a need for protrusions to search the environment (Fig. 4H,I). Furthermore, pioneer neuron protrusions projected at reduced angles, closer to the direction of migration, in comparison with those of follower FBMNs (Fig. 4J), again suggesting that the pioneer neurons are actively pathfinding. Overall, our analysis reveals that both pioneer and follower FBMNs change their behavior as the MLF overtakes

them, and, importantly, that pioneer behavior is substantially different from follower behavior, suggesting pioneer neurons may be important for guiding follower FBMNs through the hindbrain.

To examine whether the pioneer neuron is necessary for normal migration of follower FBMNs, ablation experiments were performed using *Tg(islet1:GFP)* embryos in which FBMNs are labeled with GFP. The pioneer neuron on one side of the hindbrain was ablated at 18–19 hpf, when the pioneer has just entered r5 but few or no follower FBMNs have reached r5. Unilateral ablation allowed the other side of the embryo to serve as an internal control. Analysis at 24 hpf showed that after pioneer ablation migration of follower FBMNs was disrupted with varying degrees of severity (Fig. 5A–C). DIC and fluorescent imaging immediately following ablation showed that the pioneer neuron had been killed (supplementary material Fig. S3). *In vivo* time-lapse imaging after ablation (supplementary material Movie S3) confirmed the death of the pioneer; the detritus of the ablated cell was followed in eight movies and in all cases was excluded from the neuroepithelium, either at the lateral edge or into the ventricle. Importantly, time-lapse analysis also revealed that although follower FBMNs do not migrate normally, they do remain motile. In 33% of ablated embryos we observed a ‘no migration’ phenotype, where zero to one FBMNs migrated into r6 on the manipulated side of the hindbrain (Fig. 5A,G). Furthermore, a ‘strong phenotype’ was observed in 42% of ablated embryos in which two to four neurons reach r6 (Fig. 5B,G), as well as a ‘weak phenotype’ in 25% of ablated embryos in which five to eight neurons reach r6 (Fig. 5C,G). Regardless of the severity of the phenotype, all ablated embryos exhibited an increased number of FBMNs remaining in r4 compared with controls and the few neurons able to migrate into r5 and r6 formed clumps rather than migrating individually as in controls (Fig. 5A–C). By comparison, on the unmanipulated side of the hindbrain an average of 10 neurons reached r6 by 24 hpf. Interestingly, when pioneer ablations were performed at a later stage (19–20 hpf), when several FBMNs had already reached r5, FBMN migration into r6 was similar to controls in 79% of embryos (Fig. 5G). This demonstrates that pioneer guidance is most crucial during the early phase of FBMN migration, from r4 into r5.

The migration defect after pioneer neuron ablation was still apparent at 48 hpf when FBMN migration should be complete (data not shown), confirming that the stalled migration is not merely due to developmental delay. This analysis also indicates that a follower FBMN is not generally able to rescue the migration defect. To test further the idea that a follower FBMN might share qualities of the pioneer, we ablated the second FBMN to migrate; 73% of these embryos showed normal migration (Fig. 5D,G). However, a small but consistent number of embryos with the second FBMN ablated displayed mild migration defects (Fig. 5G). This indicates that the second FBMN may have some importance in guiding FBMN migration; however, it does not appear to share the complete role or spectrum of qualities of the pioneer neuron. Finally, we wanted to control for the possibility that simply ablating any cell in the neuroepithelium during early FBMN migration could impact FBMN migration. For these experiments, we used *zCREST1:membRFP/pGFP5.3* double transgenic embryos to visualize FBMNs (red) and neuroepithelial cells in r5 (green), respectively (Fig. 5E). A single r5 neuroepithelial cell was ablated in the path of FBMN migration at 18–19 hpf. FBMN migration proceeded normally in 100% of these embryos (Fig. 5E,G), revealing that damage to the neuroepithelium is not sufficient to affect FBMN migration. In summary, these experiments provide

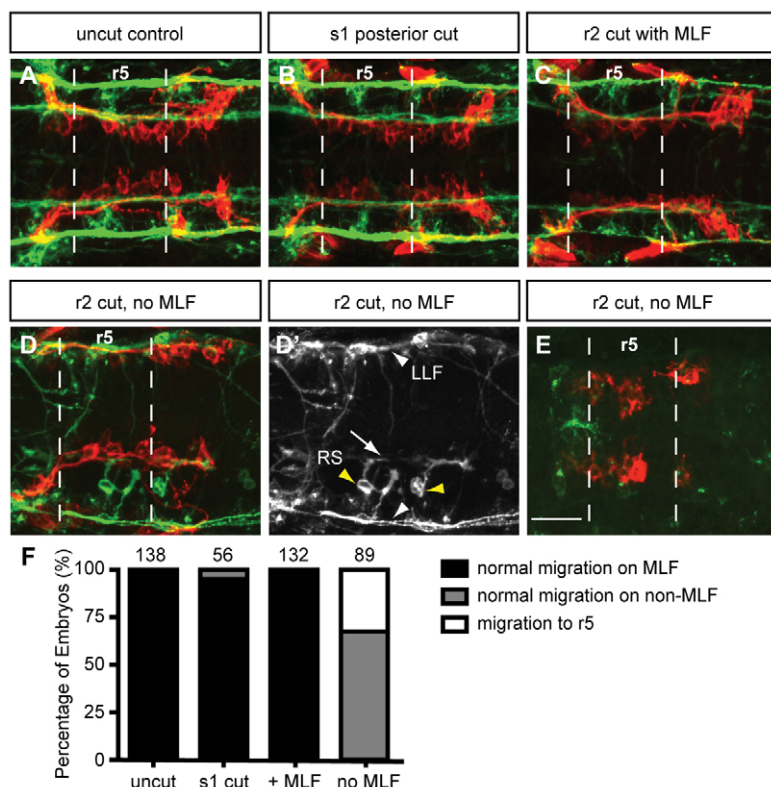


Fig. 3. Loss of MLF axons in the hindbrain blocks FBMN migration. Maximum projection dorsal views of FBMNs (red) and the MLF (green) in 22 hpf *Tg(zCREST1:membRFP)* embryos stained using zn-12 antibody. (A) Uncut control embryos at 22 hpf show that FBMNs migrate in close proximity to the MLF. (B) Cuts made posterior to the hindbrain at the first somite (s1) do not affect FBMN migration. (C) Incomplete severing at r2 allows normal MLF axon and FBMN migration. (D) Severing of the embryo at r2 often results in FBMN migration into r6 on the LLF or projections of the reticulospinal (RS) neurons. (D') zn-12 staining labels the LLF (white arrowheads), and the RS neurons (yellow arrowheads) and their projections (arrow). (E) Severing the MLF causes FBMN migration to stall in r5. (F) Percentage of embryos affected by manipulations. The number of embryos scored is indicated for each manipulation. Scale bar: 20 μ m.

evidence that the first FBMN to migrate acts as a pioneer neuron, crucial for the migration of follower FBMNs through the hindbrain.

In other contexts, pioneer neurons project axons that serve to guide axons of follower neurons during development (for a review, see Raper and Mason, 2010). We hypothesized that a similar scenario is occurring in the hindbrain, where follower FBMNs require interaction with the trailing axon of the pioneer neuron to migrate properly. To test this hypothesis, we used *Tg(zCREST1:membRFP)* embryos to visualize FBMNs and their projections (red), and ablated the trailing axon of the pioneer neuron on one side of the embryo. After axon ablation, 66% of embryos showed disruptions to FBMN migration (Fig. 5F,G). The reduced number of affected embryos after axon ablation compared with pioneer neuron ablation is likely to be due to the technical difficulty of ensuring effective targeting of the narrow axon tract. In 80% of the most severely affected axon-ablated embryos, a single neuron was found in r6 (Fig. 5F, arrowhead) that likely corresponds to the pioneer neuron. This emphasizes that these experiments specifically targeted the trailing axon, not the pioneer neuron. These experiments suggest that the interaction of follower FBMNs with the trailing axon of the pioneer neuron is crucial for follower FBMN migration.

Cdh2 is important for FBMN migration but not pioneer migration

The cell adhesion factor Cdh2 was recently shown to be important for FBMN-FBMN cohesion (Stockinger et al., 2011). Depletion of Cdh2 by morpholino (MO) injection causes stalling of FBMN migration in r4/r5, with neurons tending to coalesce at the midline (Stockinger et al., 2011). Time-lapse confocal movies of FBMN migration in *zCREST1:membRFP/HuC-GFP* double transgenic embryos depleted of Cdh2 (Fig. 6; supplementary material Movie S4) indicated that average speed and posterior velocity of follower

neurons were significantly reduced at both early and late stages of migration, consistent with an important role for Cdh2 in follower neuron migration. Interestingly, pioneer neuron average speed and posterior velocity were virtually unchanged by Cdh2 depletion (Fig. 6). Our analysis reveals that Cdh2 is important for migration of follower FBMNs but not for pioneer neuron migration.

Stockinger and colleagues (Stockinger et al., 2011) often observed one or two 'escaper' neurons in each r6 hemi-segment of Cdh2-depleted embryos; we similarly found escaper neurons in r6 in 61.5% of Cdh2-depleted embryos at 24 hpf ($n=65$). Our time-lapse imaging of Cdh2-depleted *Tg(zCREST1:membRFP/HuC-GFP)* embryos showed that 69% of the escaper neurons were pioneers (i.e. the first neuron to leave r4). The other 31% represented the second FBMN to migrate; in every instance where the second neuron escaped, a pioneer also escaped and the second neuron maintained a connection with the trailing axon of the pioneer. Interestingly, in Cdh2-depleted embryos that lack the MLF, escaper neurons were still found in r6 (supplementary material Fig. S4). We wondered whether follower FBMNs in Cdh2-depleted embryos migrate into the midline alone or by following pioneers. Time-lapse analysis showed that 50% of the time FBMNs followed a pioneer into the midline, whereas 37.5% migrated to the midline without following a pioneer. Thus, FBMNs can follow pioneer neurons into the midline, but this is not a requirement. Together, these analyses reveal that pioneer neuron migration is independent of Cdh2-mediated adhesion and is probably also independent of the MLF.

Cdh2 is important for interactions between FBMNs and axons

To determine whether Cdh2-mediated cell adhesion is required for the interaction between follower FBMNs and the trailing axon of the pioneer, we depleted Cdh2 in *Tg(zCREST1:membRFP)* embryos.

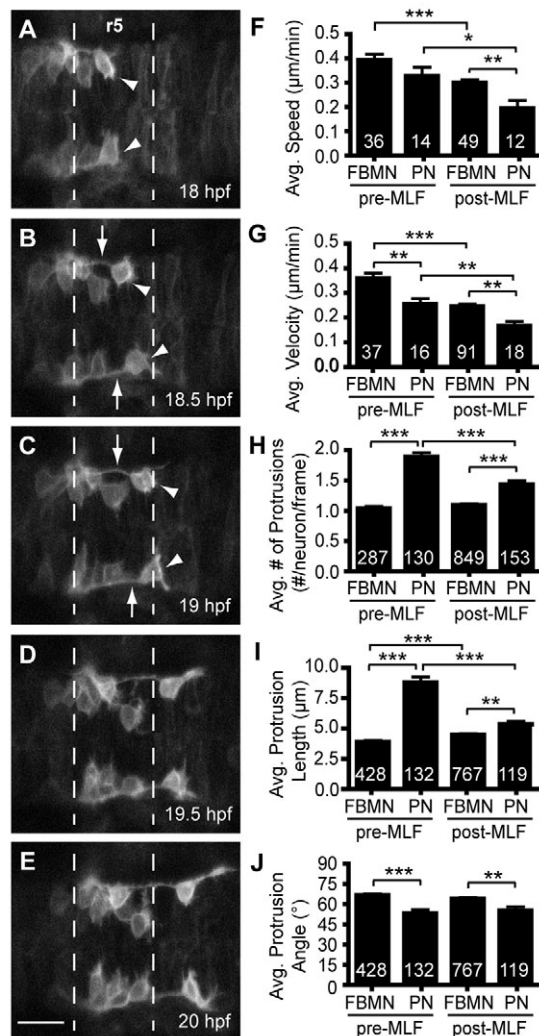


Fig. 4. The pioneer neuron behaves differently than follower FBMNs. (A-E) Still images from time-lapse imaging of Tg(zCREST1:membrRFP) embryos from 18–22 hpf shown at 30-minute intervals. Arrowheads indicate the pioneer neuron and arrows indicate the trailing axon of the pioneer neuron. (F-J) Analysis of pioneer and follower FBMN behavior before (pre-MLF) and after (post-MLF) the MLF has entered the hindbrain region. (F) Average speed of migration. (G) Average posterior velocity. (H) Average number of protrusions per neuron per 5-minute time point. (I) Average length of protrusions per 5-minute time point. (J) Average angle of protrusions, where 0° is towards the posterior in the direction of migration and 90° is towards the midline. Error bars indicate s.e.m. Significance values: * $P < 0.05$, ** $P < 0.01$, *** $P < 0.001$. Scale bar: 20 μm.

In controls, follower FBMNs, primarily the second FBMN, maintained their connection with the trailing axon of the pioneer neuron throughout FBMN migration (Fig. 7A-D). In embryos depleted of Cdh2, this interaction was absent in 62% of fixed embryos after 20 hpf ($n=181$) and in 65% of fixed embryos at 18 hpf ($n=42$; Fig. 7E-H). Time-lapse imaging of Cdh2-depleted embryos revealed similar results, where the connection between follower FBMNs and pioneers was absent in 9/12 cases during the earliest migration at 18 hpf and in 10/12 cases after 20 hpf (see supplementary material Movie S4). In these Cdh2-depleted embryos, the pioneer continued to send out projections, often long erratic projections that exit r6 laterally, but lost contact with follower

FBMNs (Fig. 7F-H). Lateral projections from r6 are reminiscent of glossopharyngeal BMNs (Chandrasekhar, 2004). However, the *islet1* regulatory elements used in our transgene do not drive expression in this neuron class (Higashijima et al., 2000; Uemura et al., 2005) and our time-lapse analyses (supplementary material Movie S4; others not shown) reveal r4-derived FBMNs migrating into this region, strongly supporting our conclusion that these laterally projecting neurons are Cdh2-deficient pioneer FBMNs. Thus, Cdh2 appears to be important for maintaining the interaction between follower FBMNs and the trailing axon of the pioneer neuron.

As the MLF is required for FBMN migration from r5 to r6, we also examined whether Cdh2-mediated adhesion is important for the interaction between FBMNs and the MLF. Depletion of Cdh2 caused FBMNs to coalesce in the midline, decreasing interactions between FBMNs and the MLF (Fig. 8A-F). High magnification images of transverse sections showed that prior to MLF axons entering r5, FBMNs are multipolar (Fig. 8G). By contrast, as the first MLF axon enters r5, FBMNs project towards the MLF (Fig. 8H,H',M). Depletion of Cdh2 resulted in decreased interaction between FBMNs and the MLF at this crucial stage, particularly when FBMNs were in the midline (Fig. 8I,I',M). This suggests that Cdh2-mediated cell adhesion is needed for the interaction between FBMNs and the MLF axon tract. In the case of the pioneer neuron, just prior to the MLF axon entering the region the pioneer extended projections in all directions (Fig. 8J). Once the MLF axon had caught up to the pioneer, the pioneer sent a single projection towards the MLF (Fig. 8K,K',M), showing that the pioneer does interact with the MLF when present, but this interaction is likely to be unimportant as the pioneer can frequently reach r6 even when the MLF is absent. Depletion of Cdh2 resulted in reduced interactions between the pioneer and the MLF in 61% of embryos (Fig. 8L,L',M), just as the MLF has appeared in the region.

DISCUSSION

In this study, we have shown that FBMNs undergo two phases of migration that are differentially regulated. First, an early phase of migration from r4 into r5, which is regulated by the ability of the first FBMN to migrate into r5 and maintain connections with follower FBMNs through its trailing axon. Second, a later phase of migration from r5 to r6, dependent upon interactions between FBMNs and the MLF. Furthermore, we have shown that Cdh2-mediated cell adhesion is important during both phases of migration for maintaining interactions between FBMNs and the trailing axon of the pioneer neuron, as well as the MLF. The pioneer neuron itself is able to migrate independently of both Cdh2 and the MLF, suggesting it uses other factors to migrate through the hindbrain.

To our knowledge, this is the first report of migration of a neuronal population that relies upon the ability of a the cell body of a single neuron to navigate through the environment and leave a trailing axon upon which succeeding neurons migrate. Only one other population, the oculomotor neurons of the midbrain, has been reported to have pioneer migratory neurons. In this case, several oculomotor neurons migrate at the same time by following long protrusions in the direction of migration (Puelles-Lobez et al., 1975; Puelles and Privat, 1977; Puelles, 1978); this differs from the case of the zebrafish FBMNs, where just one neuron on each side of the neural tube initially navigates the environment. The term 'pioneer neuron' has previously been used in the context of axon guidance rather than neuronal migration. Specifically, the pioneer has been defined as the neuron that first extends its axon to a specific target, that axon then providing a substrate upon which subsequent axons

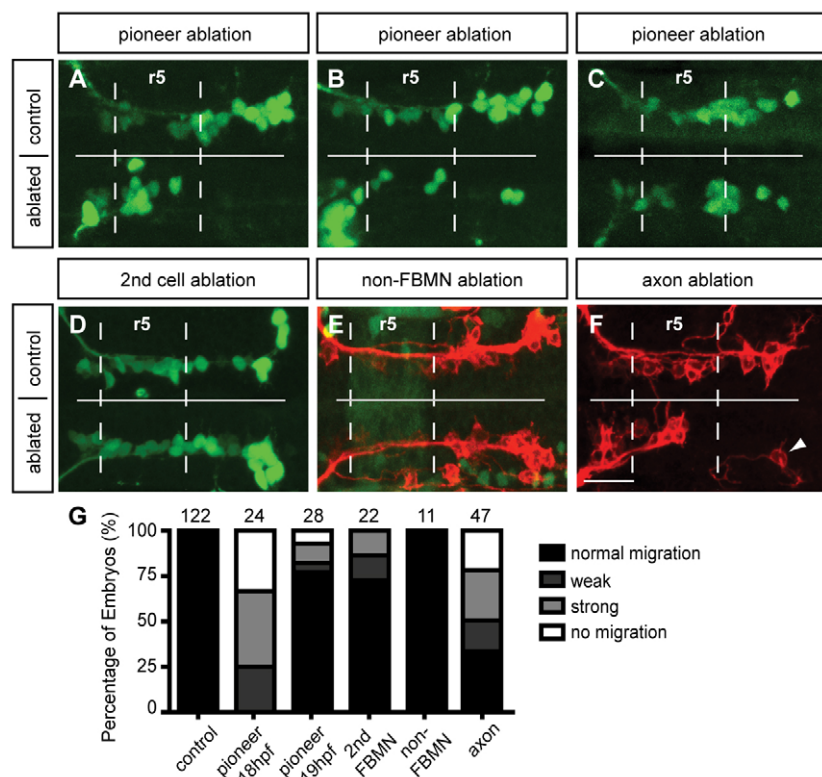


Fig. 5. Pioneer neuron ablation blocks migration of follower FBMNs. (A–C) Maximum projection images of *Tg(islet1:GFP)* (green) embryos at 24 hpf, after ablation of the pioneer neuron on one side of the embryo at 18–19 hpf. (A) Pioneer neuron ablation blocks follower FBMN migration. (B) Strong partial migration phenotype results in two to four FBMNs reaching r6. (C) Weak partial migration phenotype results in migration of five to eight FBMNs into r6. (D) Ablation of the second FBMN to migrate does not affect FBMN migration in most embryos. (E) *Tg(zCREST1:membRFP/pGFP5.3)* embryos label FBMNs (red) and neuroepithelial cells in r5 (green), respectively. Ablation of a single r5 neuroepithelial cell in the path of FBMN migration does not affect migration. (F) Ablation of the trailing axon of the pioneer neuron, using *Tg(zCREST1:membRFP)* embryos, blocks FBMN migration; arrowhead indicates presumed pioneer neuron. (G) Percentage of embryos affected by ablation. Scale bar: 20 μ m.

pathfind (Bate, 1976; Raper and Mason, 2010). Here, we have opted the term ‘pioneer’ to describe the closely related situation where the first FBMN to migrate lays down an axon tract upon which subsequent neurons navigate. Although it is the cell bodies of follower neurons that follow the pioneer axon tract, rather than axons (as in previous reports), the principle of an initial axon tract being crucial for guidance is conserved.

The zebrafish lends itself ideally to the imaging and ablation studies that have allowed us to identify pioneer FBMNs. It will be more challenging to establish whether equivalent pioneer cells function in mammalian systems. Reports of FBMN tangential migration in both the usual, caudal (posterior), direction and simultaneously in the rostral (anterior) direction in mice mutant for *Celsr1* (Qu et al., 2010) initially seem difficult to reconcile with a conserved requirement for a single pioneer neuron to lead the migration process. However, Glasco et al. (Glasco et al., 2012) recently reported that this aberrant rostral FBMN migration uses molecular mechanisms that differ from those used in caudal migration. This finding suggests the possibility that cellular mechanisms used in rostral FBMN migration may also differ from those used during normal caudal migration; thus, the existence of rostral migratory FBMNs does not *de facto* rule out the possibility that pioneer FBMNs function in mice. Nevertheless, zebrafish and murine mechanisms of FBMN migration are not always fully conserved; for example, there have been no reports of rostral FBMN migration phenotypes in zebrafish, including in the *celsr* mutants (Wada et al., 2006).

We have shown that although the first FBMN to migrate acts as a pioneer neuron, succeeding neurons do not acquire the properties of the pioneer neuron in its absence. However, ablation of the second cell to migrate does cause migration defects in a small percentage of embryos. Additionally, the second cell to migrate is able to ‘escape’ into r6 in some *Cdh2*-depleted embryos, as well as

in some MLF-blocked embryos. Although these results hint that the second neuron shares properties of the pioneer, we suggest that these findings in fact reflect the tight physical link between the pioneer and the second cell. Consistent with this idea, we have found that the second cell is only able to migrate into *Cdh2*-deficient r6 when it is in contact with the pioneer neuron. Furthermore, we suggest that the migration defects observed after ablation of the second cell are an indirect consequence of severing the link between the pioneer and follower neurons. In those cases where second cell ablation did not affect migration, it is possible that the trailing axon of the pioneer made contact with another follower FBMN, which allowed proper migration. We favor a model in which the importance of the second cell is not in having pioneer-like capacity, but rather in being the closest FBMN to the pioneer, serving to link the pioneer to follower FBMNs.

Much previous work examining FBMN migration has focused on the PCP pathway; several labs have shown that multiple components of the PCP pathway are crucial for FBMN migration both in zebrafish and in mouse (Bingham et al., 2002; Jessen et al., 2002; Carreira-Barbosa et al., 2003; Bingham et al., 2005; Wada et al., 2005; Wada et al., 2006; Rohrschneider et al., 2007; Vivancos et al., 2009; Qu et al., 2010; Walsh et al., 2011; Glasco et al., 2012). Our analysis of pioneer neurons and the MLF supports a model in which FBMN migration requires additional inputs beyond PCP signaling. We hypothesize that in the absence of contact with appropriate axon tracts, follower FBMNs are unable to respond properly to PCP signals. Although the role of the PCP pathway in pioneer neuron migration remains to be explored, we suggest that the pioneer neuron probably depends upon PCP-dependent mechanisms to migrate tangentially through the hindbrain, as neither loss of the MLF nor *Cdh2* affects its migration.

Walsh and colleagues (Walsh et al., 2011) used cell transplantation experiments to reveal a collective mode of FBMN

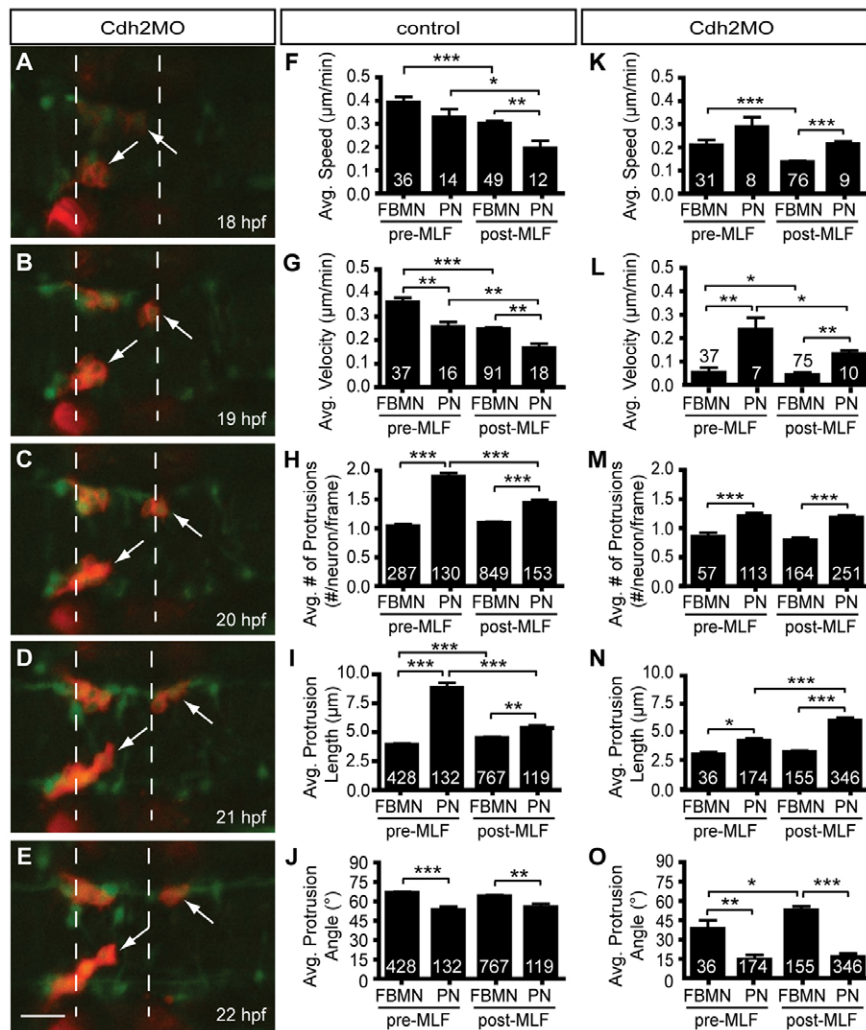


Fig. 6. Pioneer neuron migration is independent of Cdh2-mediated cell adhesion. (A-E) Still images from a representative time-lapse movie of Tg(zCREST1:membrFP/HuC-GFP) embryos injected with Cdh2MO from 18-22 hpf, shown at 1-hour intervals. Arrows indicate the pioneer neurons. (F-J) Analysis of pioneer and follower FBMN behavior before and after the MLF has entered the hindbrain region in un.injected controls. (K-O) Analysis of Cdh2MO time-lapse data comparing pioneer neuron behavior with follower FBMNs before and after the MLF is present. (F,K) Average speed. (G,L) Average posterior velocity. (H,M) Average number of protrusions per neuron per 5-minute time point. (I,N) Average protrusion length per 5-minute time point. (J,O) Average protrusion angle. Error bars indicate s.e.m. * $P < 0.05$, ** $P < 0.01$, *** $P < 0.001$. Scale bar: 20 μm.

migration that does not require cell-autonomous PCP activity but instead relies on interactions between FBMNs; PCP-deficient FBMNs can successfully migrate when they are in contact with small numbers of wild-type neurons. We have shown that in those

instances when follower FBMNs migrate in the absence of a pioneer they usually do so as small clusters of neurons, suggesting a role for collective migration. Interestingly, the ability of the pioneer neuron to navigate the environment in the absence of any

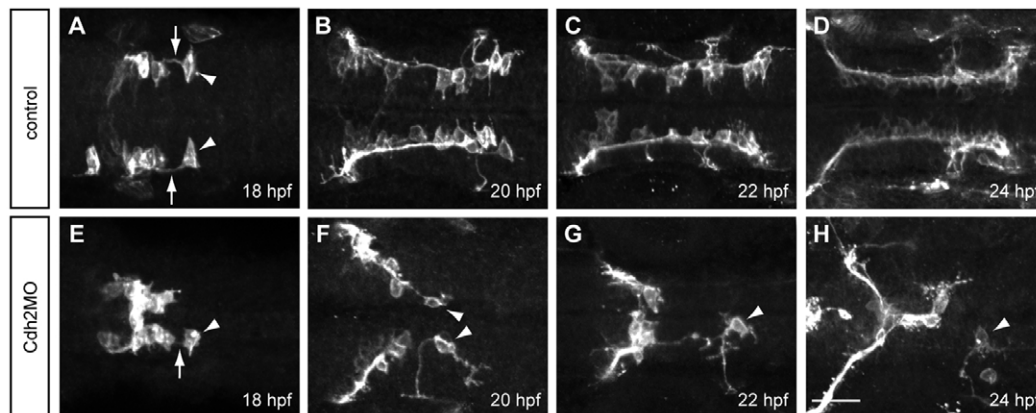


Fig. 7. Cdh2 is required for maintaining the interaction between the pioneer trailing axon and follower FBMNs. Maximum projection images of Tg(zCREST1:membrFP) embryos. (A-D) In un.injected control embryos at (A) 18 hpf, (B) 20 hpf, (C) 22 hpf and (D) 24 hpf, the trailing axon (arrows) of the pioneer neuron (arrowheads) maintains contact with follower FBMNs. (E-H) In Cdh2MO-injected embryos, the interaction between the trailing axon of the pioneer neuron and follower FBMNs is reduced or absent; examples at (E) 18 hpf, (F) 20 hpf, (G) 22 hpf and (H) 24 hpf. Arrowheads indicate the pioneer neuron. Arrow indicates the trailing axon. Scale bar: 20 μm.

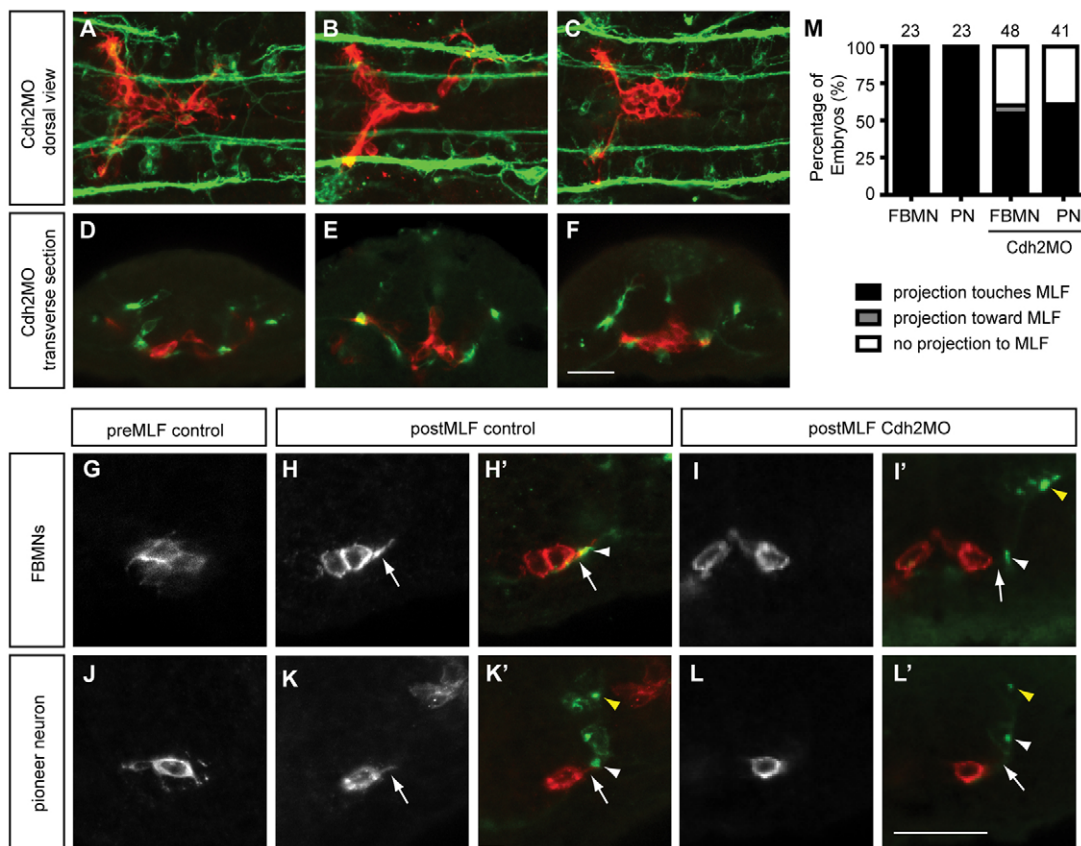


Fig. 8. Depletion of Cdh2 reduces interactions between the FBMNs and MLF. Maximum projections of Tg(zCREST1:memBRFP) embryos stained using zn-12. (A–C) Dorsal views of Cdh2MO-injected embryos at (A) 20 hpf, (B) 22 hpf and (C) 24 hpf show reduced interaction between FBMNs (red) and the MLF (green). (D–F) Transverse sections of Cdh2-depleted embryos at r5 show decreased interactions between the MLF and FBMNs at (D) 20 hpf, (E) 22 hpf and (F) 24 hpf. (G–L') High-magnification images of transverse sections at 19.5 hpf. Yellow arrowheads indicate the LLF. (G) Before the MLF is present, FBMNs send projections in random directions. (H,H') Once the MLF (white arrowhead) is present, FBMNs send a projection to the MLF (arrow). (I,I') In Cdh2-depleted embryos, FBMNs in the midline do not send projections to the MLF. (J) The pioneer neuron, before the MLF has entered r5, projects randomly. (K,K') Once the MLF is present, the pioneer neuron sends a projection towards it. (L,L') In Cdh2-depleted embryos, the pioneer has reduced interactions with the MLF. (M) Percentage of embryos with neural projections contacting the MLF. Scale bar: 20 μ m.

connection with other FBMNs highlights that pioneer neuron migration is not dependent on collective migration. A complete understanding of the interplay between collective migration and axon-dependent migration will require further experimentation.

Adhesion molecules, including Cdh2 and contactin 2 (Cntn2/Tag1), are also important for FBMN migration within the hindbrain (Sittaramane et al., 2009; Stockinger et al., 2011). Sittaramane et al. (Sittaramane et al., 2009) found that Cntn2-deficient specimens have defects in FBMN migration. Interestingly, as well as being expressed in FBMNs, Cntn2 protein is expressed on the MLF and is crucial for MLF fasciculation and pathfinding (Wolman et al., 2008). In preliminary Cntn2-depletion experiments (S.J.W. and V.E.P., unpublished), we find that FBMN migration defects are typically accompanied by MLF defects; we therefore suggest that Cntn2 may play an important role in interactions between the MLF and FBMNs.

Stockinger and colleagues (Stockinger et al., 2011) recently reported that Cdh2-deficient specimens also have defects in FBMN migration. They attributed these migration defects to reduced cohesion between neuroepithelial cells of the neural tube, which normally acts to restrict apical FBMN migration. These authors were unable to test directly whether Cdh2 functions within FBMNs

because cell transplantation experiments designed to test cell autonomy of Cdh2 function instead result in cell sorting; our own attempts at this approach were similarly unsuccessful. Nevertheless, Stockinger et al. (Stockinger et al., 2011) dismissed a role for Cdh2 in direct regulation of FBMN cohesion on the basis that 'escaper' FBMNs migrate out of r4 in the absence of Cdh2 function. Our results clarify that the 'escapers' are pioneer neurons with different migratory properties from other FBMNs. Furthermore, our data reveal a role for Cdh2 early in FBMN migration, when it is important for interactions between follower FBMNs and the trailing axon of the pioneer neuron. We suggest that the loss of contact between follower FBMNs and the pioneer may in part lead to the migration defects observed in Cdh2-depleted embryos. Additionally, we have shown that Cdh2 is important for the interaction between the MLF and FBMNs; when Cdh2 is depleted, this interaction is reduced allowing FBMNs to migrate towards the midline. In summary, although a role for Cdh2 in controlling adhesion of neuroepithelial cells probably contributes to the FBMN migration defects found in Cdh2-depleted embryos (Stockinger et al., 2011), our data support a model in which Cdh2-mediated cohesion between FBMNs and between FBMNs and the MLF are also crucial for the migration process.

Acknowledgements

We thank Vytas Bindokas of the University of Chicago Integrated Microscopy Core for help with ablation experiments, and Robert Ho and Joanna Rowell for comments on the manuscript.

Funding

This work was supported by a National Institutes of Health (NIH) fellowship [F32 HD069117 to S.J.W.], by a March of Dimes grant [FY07-410 to V.E.P.], by the National Science Foundation (NSF) Major Research Instrumentation grant [1040297] and by The University of Chicago Clinical and Translational Science Award (CTSA) [UL1 RR024999]. Deposited in PMC for release after 12 months.

Competing interests statement

The authors declare no competing financial interests.

Supplementary material

Supplementary material available online at <http://dev.biologists.org/lookup/suppl/doi:10.1242/dev.087148/-/DC1>

References

- Bate, C. M. (1976). Pioneer neurones in an insect embryo. *Nature* **260**, 54–56.
- Bingham, S., Higashijima, S., Okamoto, H. and Chandrasekhar, A. (2002). The Zebrafish trilobite gene is essential for tangential migration of branchiomotor neurons. *Dev. Biol.* **242**, 149–160.
- Bingham, S. M., Toussaint, G. and Chandrasekhar, A. (2005). Neuronal development and migration in zebrafish hindbrain explants. *J. Neurosci. Methods* **149**, 42–49.
- Carreira-Barbosa, F., Concha, M. L., Takeuchi, M., Ueno, N., Wilson, S. W. and Tada, M. (2003). Prickle 1 regulates cell movements during gastrulation and neuronal migration in zebrafish. *Development* **130**, 4037–4046.
- Chandrasekhar, A. (2004). Turning heads: development of vertebrate branchiomotor neurons. *Dev. Dyn.* **229**, 143–161.
- Chitnis, A. B. and Kuwada, J. Y. (1990). Axonogenesis in the brain of zebrafish embryos. *J. Neurosci.* **10**, 1892–1905.
- Gänzler-Odenthal, S. I. and Redies, C. (1998). Blocking N-cadherin function disrupts the epithelial structure of differentiating neural tissue in the embryonic chicken brain. *J. Neurosci.* **18**, 5415–5425.
- Garel, S., Garcia-Dominguez, M. and Charnay, P. (2000). Control of the migratory pathway of facial branchiomotor neurones. *Development* **127**, 5297–5307.
- Glasco, D. M., Sittaramane, V., Bryant, W., Fritzsche, B., Sawant, A., Paudyal, A., Stewart, M., Andre, P., Cadete Vilhais-Neto, G., Yang, Y. et al. (2012). The mouse Wnt/PCP protein Vangl2 is necessary for migration of facial branchiomotor neurons, and functions independently of Dishevelled. *Dev. Biol.* **369**, 211–222.
- Grant, P. K. and Moens, C. B. (2010). The neuroepithelial basement membrane serves as a boundary and a substrate for neuron migration in the zebrafish hindbrain. *Neural Dev.* **5**, 9.
- Hatta, C. B. and Takeichi, M. (1986). Expression of N-cadherin adhesion molecules associated with early morphogenetic events in chick development. *Nature* **320**, 447–449.
- Hatten, M. E. (1999). Central nervous system neuronal migration. *Annu. Rev. Neurosci.* **22**, 511–539.
- Hernández-Montiel, H. L., Meléndez-Herrera, E., Cepeda-Nieto, A. C., Mejía-Viggiano, C., Larriva-Sahd, J., Guthrie, S. and Varela-Echavarría, A. (2003). Diffusible signals and fasciculated growth in reticulospinal axon pathfinding in the hindbrain. *Dev. Biol.* **255**, 99–112.
- Higashijima, S., Hotta, Y. and Okamoto, H. (2000). Visualization of cranial motor neurons in live transgenic zebrafish expressing green fluorescent protein under the control of the islet-1 promoter/enhancer. *J. Neurosci.* **20**, 206–218.
- Hong, E. and Brewster, R. (2006). N-cadherin is required for the polarized cell behaviors that drive neurulation in the zebrafish. *Development* **133**, 3895–3905.
- Jessen, J. R., Topczewski, J., Bingham, S., Sepich, D. S., Marlow, F., Chandrasekhar, A. and Solnica-Krezel, L. (2002). Zebrafish trilobite identifies new roles for Strabismus in gastrulation and neuronal movements. *Nat. Cell Biol.* **4**, 610–615.
- Kimmel, C. B., Powell, S. L. and Metcalfe, W. K. (1982). Brain neurons which project to the spinal cord in young larvae of the zebrafish. *J. Comp. Neurol.* **205**, 112–127.
- Kimmel, C. B., Hatta, K. and Metcalfe, W. K. (1990). Early axonal contacts during development of an identified dendrite in the brain of the zebrafish. *Neuron* **4**, 535–545.
- Kimmel, C. B., Ballard, W. W., Kimmel, S. R., Ullmann, B. and Schilling, T. F. (1995). Stages of embryonic development of the zebrafish. *Dev. Dyn.* **203**, 253–310.
- Lele, Z., Folchert, A., Concha, M., Rauch, G. J., Geisler, R., Rosa, F., Wilson, S. W., Hamersmiedt, M. and Bally-Cuif, L. (2002). parachute/n-cadherin is required for morphogenesis and maintained integrity of the zebrafish neural tube. *Development* **129**, 3281–3294.
- Mapp, O. M., Wanner, S. J., Rohrschneider, M. R. and Prince, V. E. (2010). Prickle1b mediates interpretation of migratory cues during zebrafish facial branchiomotor neuron migration. *Dev. Dyn.* **239**, 1596–1608.
- Mendelson, B. (1986). Development of reticulospinal neurons of the zebrafish. II. Early axonal outgrowth and cell body position. *J. Comp. Neurol.* **251**, 172–184.
- Metcalfe, W. K., Myers, P. Z., Trevarrow, B., Bass, M. B. and Kimmel, C. B. (1990). Primary neurons that express the L2/HNK-1 carbohydrate during early development in the zebrafish. *Development* **110**, 491–504.
- Nadarajah, B. and Parnavelas, J. G. (2002). Modes of neuronal migration in the developing cerebral cortex. *Nat. Rev. Neurosci.* **3**, 423–432.
- Park, H. C., Kim, C. H., Bae, Y. K., Yeo, S. Y., Kim, S. H., Hong, S. K., Shin, J., Yoo, K. W., Hibi, M., Hirano, T. et al. (2000). Analysis of upstream elements in the HuC promoter leads to the establishment of transgenic zebrafish with fluorescent neurons. *Dev. Biol.* **227**, 279–293.
- Picker, A., Scholpp, S., Böhl, H., Takeda, H. and Brand, M. (2002). A novel positive transcriptional feedback loop in midbrain-hindbrain boundary development is revealed through analysis of the zebrafish pax2.1 promoter in transgenic lines. *Development* **129**, 3227–3239.
- Prince, V. E., Joly, L., Ekker, M. and Ho, R. K. (1998). Zebrafish hox genes: genomic organization and modified colinear expression patterns in the trunk. *Development* **125**, 407–420.
- Puelles-Lobez, L., Malagon-Cobos, F. and Génis-Galvez, J. M. (1975). The migration of oculomotor neuroblasts across the midline in the chick embryo. *Exp. Neurol.* **47**, 459–469.
- Puelles, L. (1978). A Golgi-study of oculomotor neuroblasts migrating across the midline in chick embryos. *Anat. Embryol. (Berl.)* **152**, 205–215.
- Puelles, L. and Privat, A. (1977). Do oculomotor neuroblasts migrate across the midline in the retinal rat brain? *Anat. Embryol. (Berl.)* **150**, 187–206.
- Qu, Y., Glasco, D. M., Zhou, L., Sawant, A., Ravn, A., Fritzsche, B., Damrau, C., Murdoch, J. N., Evans, S., Pfaff, S. L. et al. (2010). Atypical cadherins Celsr1–3 differentially regulate migration of facial branchiomotor neurons in mice. *J. Neurosci.* **30**, 9392–9401.
- Radice, G. L., Rayburn, H., Matsunami, H., Knudsen, K. A., Takeichi, M. and Hynes, R. O. (1997). Developmental defects in mouse embryos lacking N-cadherin. *Dev. Biol.* **181**, 64–78.
- Raper, J. and Mason, C. (2010). Cellular strategies of axonal pathfinding. *Cold Spring Harb. Perspect. Biol.* **2**, a001933.
- Rohrschneider, M. R., Elsen, G. E. and Prince, V. E. (2007). Zebrafish Hoxb1a regulates multiple downstream genes including prickle1b. *Dev. Biol.* **309**, 358–372.
- Ross, M. E. and Walsh, C. A. (2001). Human brain malformations and their lessons for neuronal migration. *Annu. Rev. Neurosci.* **24**, 1041–1070.
- Ross, L. S., Parrett, T. and Easter, S. S., Jr (1992). Axonogenesis and morphogenesis in the embryonic zebrafish brain. *J. Neurosci.* **12**, 467–482.
- Sittaramane, V., Sawant, A., Wolman, M. A., Maves, L., Halloran, M. C. and Chandrasekhar, A. (2009). The cell adhesion molecule Tag1, transmembrane protein Stbm/Vangl2, and Lamininalpha1 exhibit genetic interactions during migration of facial branchiomotor neurons in zebrafish. *Dev. Biol.* **325**, 363–373.
- Song, M. R. (2007). Moving cell bodies: understanding the migratory mechanism of facial motor neurons. *Arch. Pharm. Res.* **30**, 1273–1282.
- Stockinger, P., Maitre, J. L. and Heisenberg, C. P. (2011). Defective neuroepithelial cell cohesion affects tangential branchiomotor neuron migration in the zebrafish neural tube. *Development* **138**, 4673–4683.
- Uemura, O., Okada, Y., Ando, H., Guedj, M., Higashijima, S., Shimazaki, T., Chino, N., Okano, H. and Okamoto, H. (2005). Comparative functional genomics revealed conservation and diversification of three enhancers of the is1 gene for motor and sensory neuron-specific expression. *Dev. Biol.* **278**, 587–606.
- Valiente, M. and Marín, O. (2010). Neuronal migration mechanisms in development and disease. *Curr. Opin. Neurobiol.* **20**, 68–78.
- Vivancos, V., Chen, P., Spassky, N., Qian, D., Dabdoub, A., Kelley, M., Studer, M. and Guthrie, S. (2009). Wnt activity guides facial branchiomotor neuron migration, and involves the PCP pathway and JNK and ROCK kinases. *Neural Dev.* **4**, 7.
- Wada, H. and Okamoto, H. (2009a). Roles of noncanonical Wnt/PCP pathway genes in neuronal migration and neurulation in zebrafish. *Zebrafish* **6**, 3–8.
- Wada, H. and Okamoto, H. (2009b). Roles of planar cell polarity pathway genes for neural migration and differentiation. *Dev. Growth Differ.* **51**, 233–240.
- Wada, H., Iwasaki, M., Sato, T., Masai, I., Nishiwaki, Y., Tanaka, H., Sato, A., Nojima, Y. and Okamoto, H. (2005). Dual roles of zygotic and maternal Scribble1 in neural migration and convergent extension movements in zebrafish embryos. *Development* **132**, 2273–2285.
- Wada, H., Tanaka, H., Nakayama, S., Iwasaki, M. and Okamoto, H. (2006). Frizzled3a and Celsr2 function in the neuroepithelium to regulate migration of facial motor neurons in the developing zebrafish hindbrain. *Development* **133**, 4749–4759.
- Walsh, G. S., Grant, P. K., Morgan, J. A. and Moens, C. B. (2011). Planar polarity pathway and Nance-Horan syndrome-like 1b have essential cell-autonomous functions in neuronal migration. *Development* **138**, 3033–3042.
- Wolman, M. A., Sittaramane, V. K., Essner, J. J., Yost, H. J., Chandrasekhar, A. and Halloran, M. C. (2008). Transient axonal glycoprotein-1 (TAG-1) and laminin-alpha1 regulate dynamic growth cone behaviors and initial axon direction in vivo. *Neural Dev.* **3**, 6.

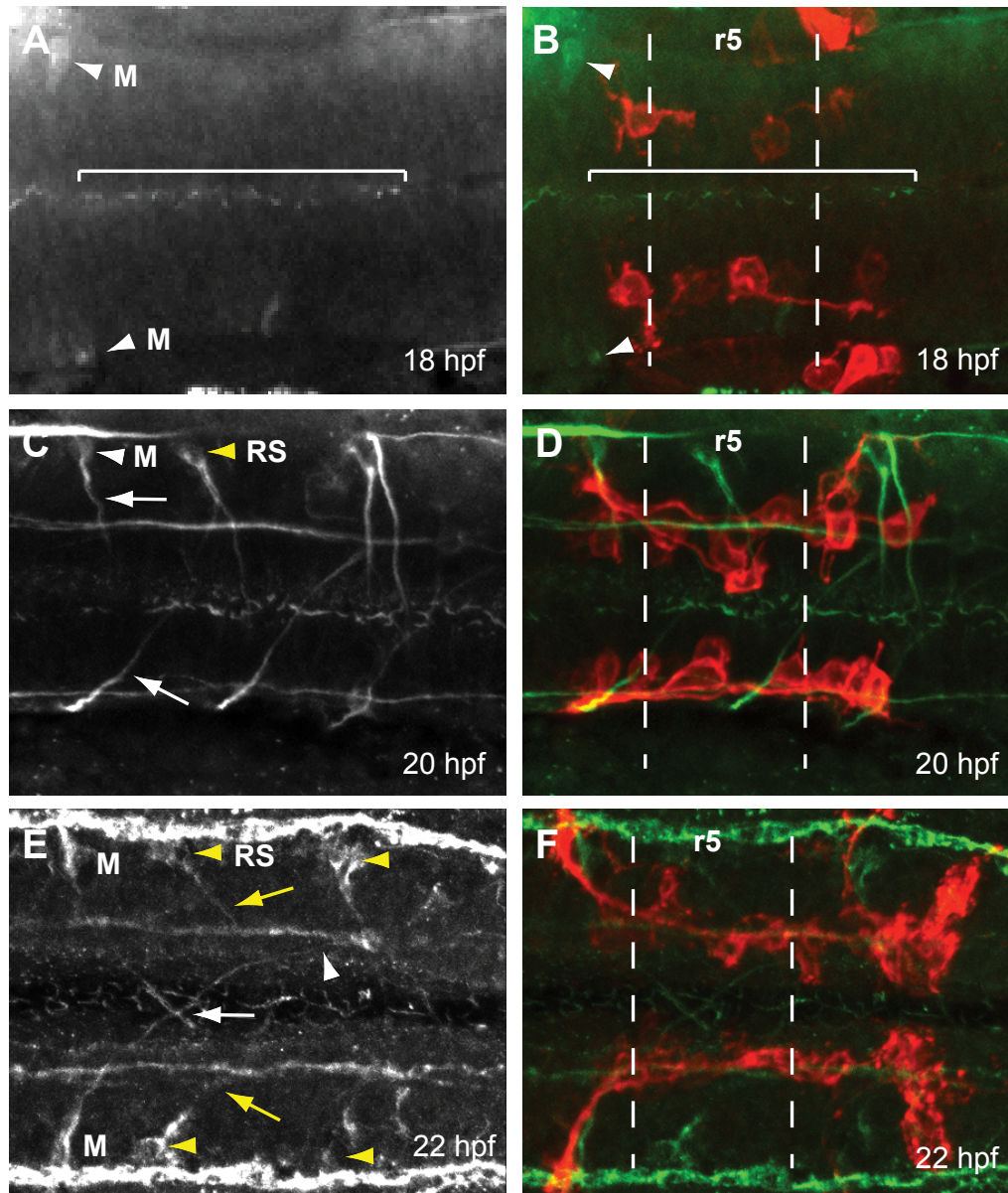


Fig. S1. Early FBMN migration into r5 and r6 precedes both Mauthner and reticulospinal neuron axon projection into the hindbrain. Maximum projection dorsal views of Tg(*zCREST*:membRFP) embryos immunostained with an acetylated tubulin antibody (A,C,E) and merged images (green; B,D,F). (A,B) At 18 hpf, Mauthner (M) neuron cell bodies are present in r4 (white arrowhead) but their axons are not yet present. Cilia in the lumen of the hindbrain (bracket) as well as stereocilia in the otic vesicle (not shown) are present at this stage, verifying antibody staining efficacy. (C,D) At 20 hpf, axons of the Mauthner neurons have begun to project towards the hindbrain midline (white arrow). Additionally, reticulospinal (RS) neuron cell bodies are present (yellow arrowhead) and have begun to project their axons toward the MLF. (E,F) At 22 hpf the axons of the Mauthner neurons have crossed at the midline in r5 (white arrow) and will soon contribute to the MLF axon tract (white arrowhead). RS neurons (yellow arrowhead) have sent out projections that have contributed to the MLF (yellow arrow).

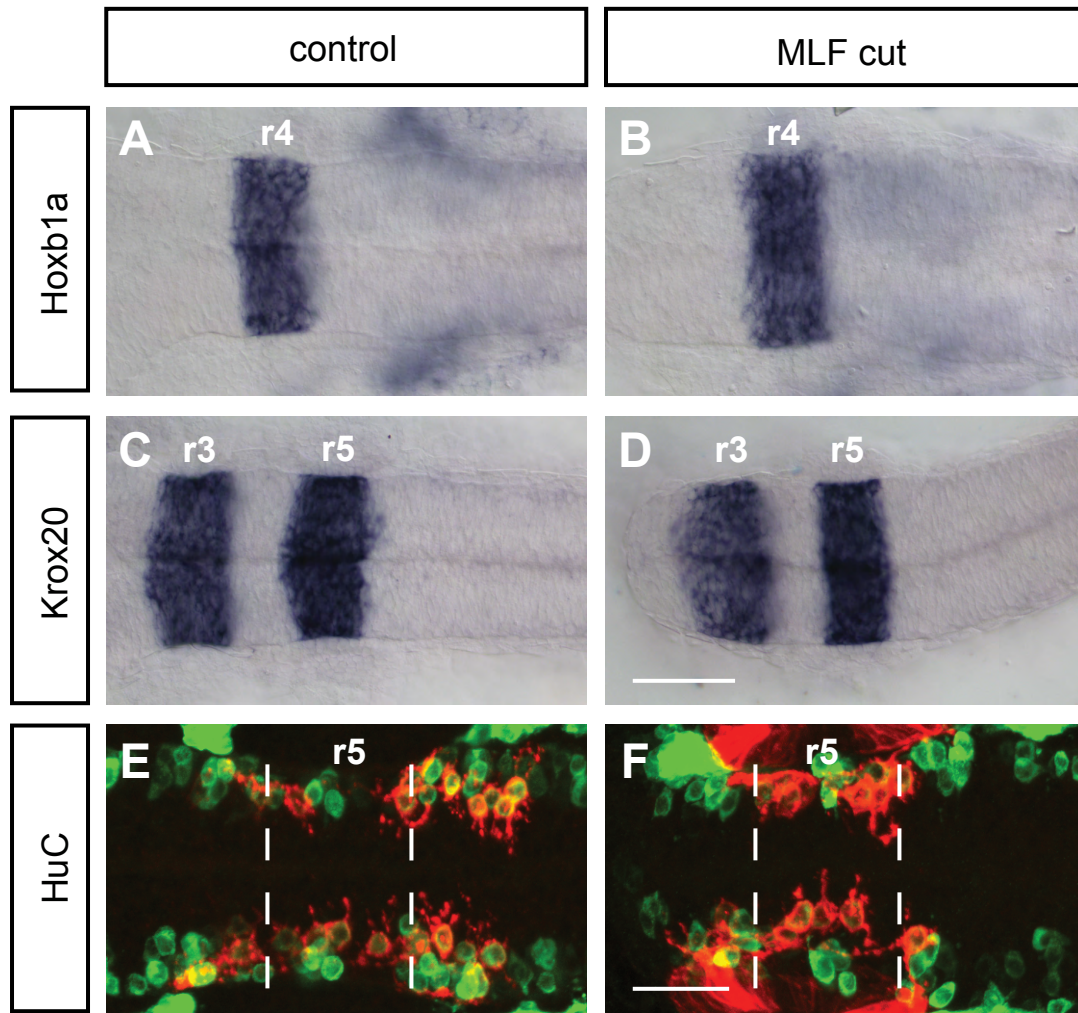


Fig. S2. Blocking the MLF does not affect the organization of the hindbrain. (A-D) *In situ* hybridization of anterior-posterior markers in control and MLF-blocked embryos at 24 hpf. (A,B) *hoxb1a* expression in r4 is unaffected in embryos lacking MLF axons (B) compared with controls (A). (C,D) *krox20* expression in r3 and r5 is unaffected in embryos lacking MLF axons (D) compared with controls (C). (E,F) HuC antibody staining in *zCREST1:memBRFP* transgenic embryos at 24 hpf. (F) HuC-labeled neuron number (green) is not affected by blocking MLF axons (F); however, the localization of these neurons is somewhat disorganized compared with controls (E). Dashed lines indicate r5 boundaries. Scale bars: 50 μ m for A-D; 20 μ m for E,F.

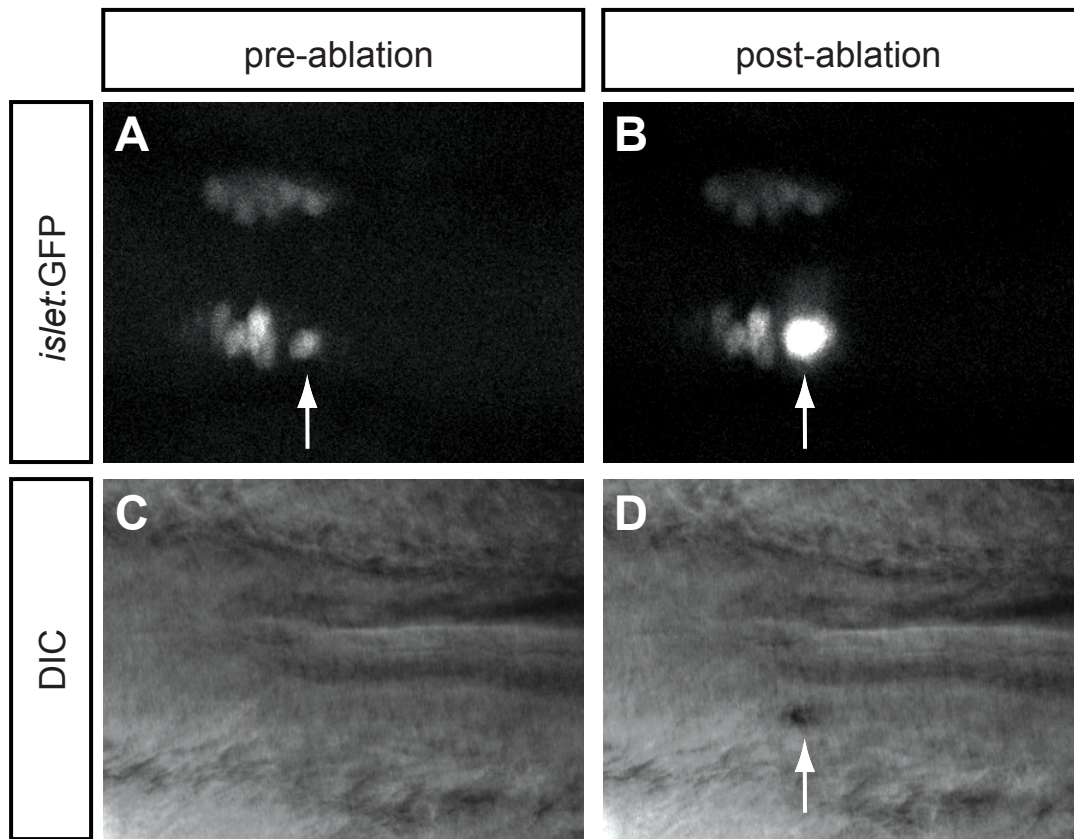


Fig. 3. Laser ablation effectively kills the pioneer neuron. (A,B) Dorsal views of a Tg(*islet:GFP*) embryo (A) before and (B) immediately after ablation of the pioneer neuron (arrow). (C,D) DIC imaging of the same embryo (C) before and (D) immediately after ablation of the pioneer neuron. (B,D) Arrows indicate that the pioneer neuron has indeed been killed by the ablation.

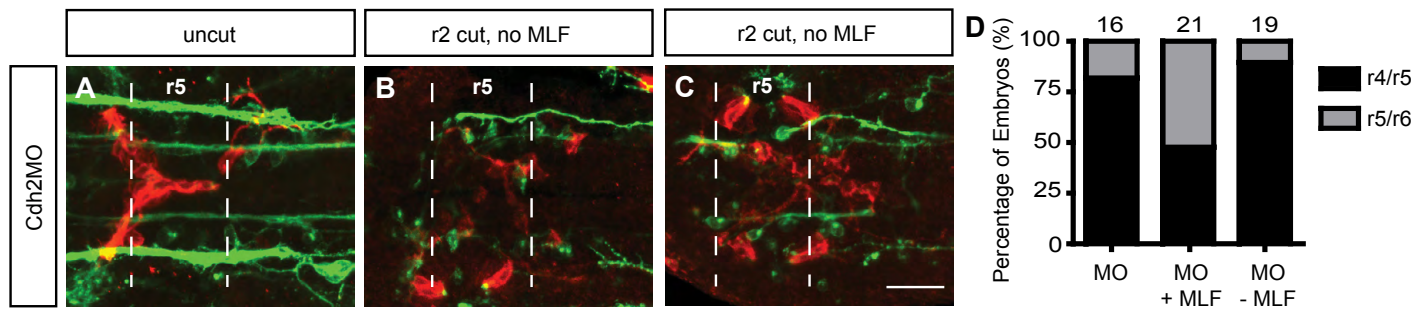
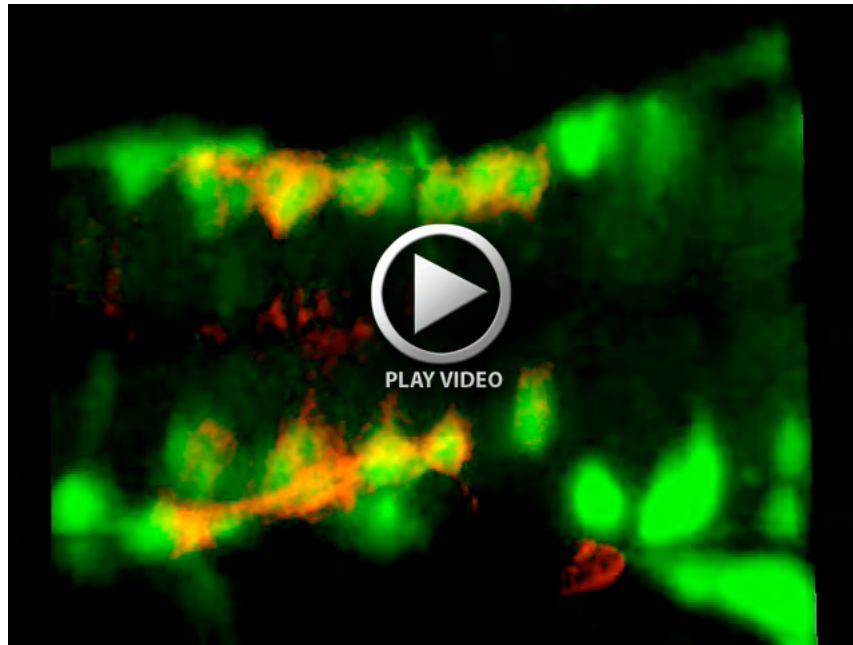
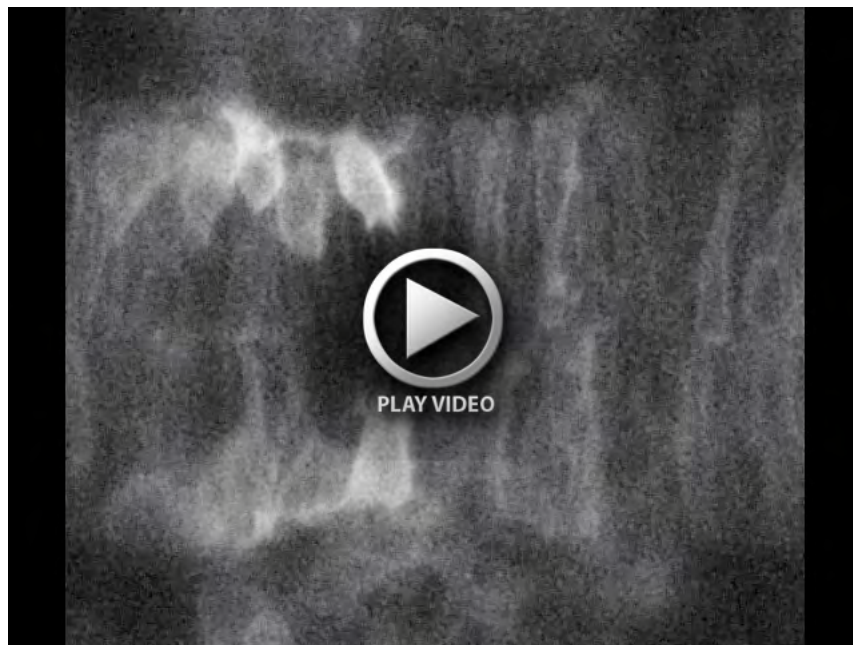


Fig. S4. Loss of both Cdh2 and MLF axons in the hindbrain blocks FBMN migration. (A-C) Maximum projection dorsal views of FBMNs (red) and the MLF (green) in 24 hpf Cdh2-depleted Tg(*zCREST1*:memBRFP) zebrafish embryos stained with zn-12 antibody. In all treatments, FBMNs coalesce in the midline; however, FBMNs never migrate along either the LLF or projections of the reticulospinal neurons. Broken lines highlight r5 boundaries. (A) Uncut control Cdh2-depleted embryos at 24 hpf show typical Cdh2-depletion phenotype of FBMN migration into r5 and coalescence of neurons in the midline. In a smaller proportion of Cdh2-depleted embryos, FBMNs still coalesce at the midline but are able to migrate into r6. (B) In embryos lacking both Cdh2 and the MLF, the majority of embryos show FBMNs that migrate only into r5. (C) In a smaller number of embryos lacking both Cdh2 and the MLF, FBMNs migrate into r6. (D) Percentage of embryos affected by Cdh2 depletion and severing manipulations. Cdh2 depletion alone (MO) results in 82% of embryos exhibiting stalled FBMN migration in r5 and 18% with FBMNs migrating into r6. In Cdh2-depleted embryos in which the embryos were severed incompletely so the MLF is still present (MO +MLF), 48% of embryos show stalled migration in r5, whereas 52% of embryos show FBMN migration reaching r6. In embryos depleted of both Cdh2 and the MLF (MO -MLF), 89% result in FBMNs stalling in r5 and 11% result in FBMNs reaching r6. The number of embryos scored is indicated. Scale bar: 20 μ m.



Movie 1. FBMN migration into r5/r6 occurs prior to the presence of the MLF. Time-lapse movie of a *zCREST1:membRFP/HuC-GFP* double transgenic embryo from 18-20 hpf. Z-stacks were taken at 5-minute intervals. FBMNs (red) migrate from r4 into r5 before the first MLF axon (green) enters the r4-r6 hindbrain region.

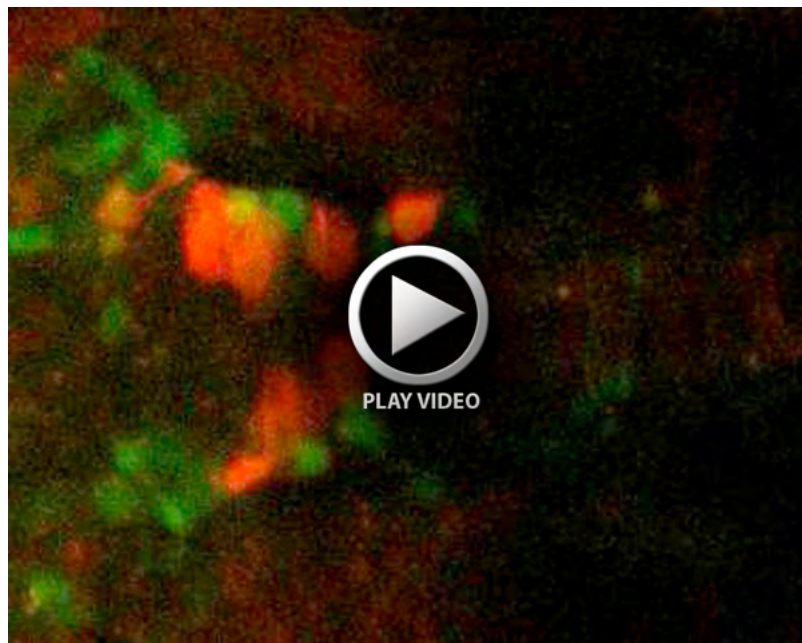


Movie 2. The first FBMN to migrate navigates the environment. Time-lapse movie of a *zCREST1:membRFP* transgenic embryo from 18-20 hpf. Z-stacks were taken at 5-minute intervals. The first FBMN to migrate proceeds ahead of the following FBMNs, leaves behind a trailing axon and sends out many protrusions in the direction of migration.



Movie 3. Ablation of the pioneer neuron blocks FBMN migration into r5 but does not affect FBMN motility.

Time-lapse movie of a *zCREST1:membRFP* transgenic embryo taken from 19-20 hpf after ablation of the pioneer neuron. Z-stacks were taken at 5-minute intervals. Ablation of the pioneer neuron blocks FBMN migration into r5; however, FBMNs are still motile. The detritus of the ablated cell was followed in all eight pioneer ablation time-lapse movies obtained and it was always excluded from the neuroepithelium, either at the lateral edge or into the ventricle (as observed in this movie).



Movie 4. Cdh2 depletion affects FBMN migration, but not pioneer migration. Time-lapse movie of a *zCREST1:membRFP/HuC-GFP* double transgenic embryo injected with Cdh2MO taken from 18-22 hpf. Z-stacks were taken at 5-minute intervals. FBMNs (red) migrate from r4 into r5 before the first MLF axon (green) enters the r4-r6 hindbrain region. The top FBMN chain shows the migration of most FBMNs stalls in r5, whereas a pioneer neuron and a second FBMN escape into r6. Bottom FBMN chain shows Cdh2-depleted FBMN migration into the r5 midline.